



University
of Glasgow

Domingo-Roca, R., Jackson, J.C. and Windmill, J.F.C. (2017) Bioinspired 3D-printed Piezoelectric Device for Acoustic Frequency Separation. In: IEEE Sensors 2017, Glasgow, UK, 30 Oct - 01 Nov 2017, ISBN 9781509010127.

There may be differences between this version and the published version. You are advised to consult the publisher's version if you wish to cite from it.

<http://eprints.gla.ac.uk/174940/>

Deposited on: 11 December 2018

Enlighten – Research publications by members of the University of Glasgow_
<http://eprints.gla.ac.uk>

Bioinspired 3D-printed piezoelectric device for acoustic frequency separation

R. Domingo-Roca, J. C. Jackson, J. F. C. Windmill

Centre for Ultrasonic Engineering, Electronic & Electrical Engineering Dept.,
Bioacoustics Group, University of Strathclyde
Glasgow, Scotland, United Kingdom
roger.domingo-roca@strath.ac.uk

Abstract — Development of 3D-printed devices, sensors, and actuators has become increasingly popular in recent years due to low cost, rapid production, and device personalization. This personalization process allows development of devices with unique physical properties and phenomena that enhance the desired properties of the 3D-printed part. Biomimetics is a commonly used technique to develop 3D-printed devices, as organisms present in nature can provide smart and simple solutions to complex problems across a wide range of applications. Locust ears have a simple tympanic membrane with varying thicknesses that allows frequency selection, as well as presenting nonlinear phenomena. This acoustic frequency selection assists the insect in predation and swarming. In this work we present the development of a polymeric material that has been used to 3D-print a frequency selective piezoelectric sensor inspired by the locust's tympanic membrane. 3D-printing of functional sensors and/or actuators provides an insight into the development and enhancement of polymer-based science, with exciting and promising potential for the near future.

Keywords—Piezoelectric; polymer; 3D printing; locust; biomimesis

I. INTRODUCTION

Biomimesis has become a very common tool during recent years, not only in science where it is used to develop new systems, devices, and materials [1, 2], but also in fields like architecture or art [3]. Taking inspiration from natural systems has allowed scientists to develop new aerodynamic systems [4], robots with specific capabilities [5], and new materials with unique properties [1, 2], among others. One of the rising areas of research into biomimetic systems and devices is the acoustical engineering field [6], not only to develop microphones and loudspeakers inspired by biological systems, but also to develop signal processing systems, hearing aid devices, and other biomedical applications [7-9]. One of the most studied acoustic systems is the locust's tympanum membrane (TM), consisting of a pear-shaped membrane of variable thickness that responds to low frequencies in its thick region, and to high frequencies in its thin region. This ear membrane also reveals the presence of travelling waves and other nonlinear effects like distortion product otoacoustic emissions (DPOAEs) [10, 11].

Development of micro-devices demands small and complex structures that can be built rapidly and at low cost. Typically the most common polymer-based microelectromechanical systems (MEMS) approaches are slow and time consuming.

Three dimensional (3D) printing techniques permit the rapid production of complex and accurate geometries from computer aided design (CAD) files. One of the disadvantages of additive manufacturing, though, is that the resulting parts are epoxy- or polymer-based, reducing their functionality to be solely dependent on their mechanical and geometric properties. Nevertheless, when adding highly functional materials to these plastics, the resulting composite material can become useful for a wider range of applications, such as conductivity, piezoelectricity, and magnetism.

The aim of this work is to develop a 3D-printable polymer-based material that can be used to build a frequency-selective bioinspired system, consisting of a simple reconstruction of the locust's TM, and use this technique as an alternative to the most typical and commonly used MEMS methods.

II. MATERIALS AND METHODS

The experiments reported in this paper used polyvinylidene fluoride (PVDF) films of 110 μm thickness (Precision Acoustics), bisphenol-A ethoxylate dimethacrylate (BEMA), PlasWhite (Asiga), phenylbis (2,4,6-trimethylbenzoyl) phosphine oxide (Irgacure 819), and SUDAN I (Sigma Aldrich).

A. Synthesis of the polymeric matrices

The synthesized polymeric matrix was developed by mixing BEMA with Irgacure 819 at 1wt%. The mixture was left under magnetic stirring for 24 hours. Then, 0.1 wt% of SUDAN I was added into the mixture with respect to BEMA and the mixture was put in a THINKY AER-250 mechanical mixer, mixing the composite for 3 minutes at 1500 rpm, and de-foaming it for 2 minutes at 1200 rpm. After mechanical mixing and sonication for 5 minutes, a control BEMA sample was made using a screen printing technique, with a layer thickness of 50 μm , using an RK control coater. Every layer was cured under UV light for one minute using an Intertronics IUUV250 Hand Lamp (Intertronics, Kidlington, England, UK).

The mixture was used with an ASIGA PicoPlus27 3D printer (ASIGA, Anaheim Hills, California, USA) and 3D-printed at 10 μm slice thickness. Firstly, a support structure (30 mm long, 7 mm wide, 1 mm wall thickness, and 1 mm height) was 3D-printed using PlasWhite, and the BEMA was 3D-printed onto it afterwards. The 3D-printed sample was 30 mm long, 7 mm wide, and has two well-differentiated thickness regions of 1.2 mm and 2 mm, with the thicker region having a

length of 11.5 mm (sample 1). Once the sample was successfully 3D-printed, two PVDF layers were attached onto it, one on top of each region, in order to provide an electrical output corresponding to the vibration of the 3D-printed layers. The full structure was glued onto a glass slide (see Fig. 1a). A second sample of variable thickness of 2 mm to 1 mm was printed, as shown in Fig. 1.

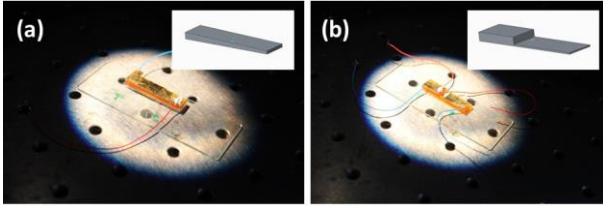


Fig. 1. (a) Shows the sample with variable thickness and its corresponding CAD file, and (b) shows the sample with two well differentiated regions with different thicknesses and its corresponding CAD file.

III. EXPERIMENTAL RESULTS

A. Mechanical properties

The mechanical properties of the developed material were evaluated using an MFT 3D Nanoindenter. Force displacement load-unload curves were measured using a calibrated Berkovich tip made of single crystalline diamond. The reduced Young's modulus (E_r) and the hardness (H) values were evaluated using the method of Oliver and Pharr [12]. The tests consisted in arrays of 6x6 indents, separated from each other by 15 μm and covering a total area of 90 μm^2 . This separation between indents was imposed to avoid the influence of neighbour indentations. The maximum applied load was of 100 μN . The average Young's modulus (E) and H measured values were 3.070 ± 0.010 MPa, and 744.21 ± 5.40 kPa respectively, which are in accordance with previous studies [13]. The mechanical response of the 3D-printed polymer is shown in Fig. 2, revealing a purely elastic behaviour.

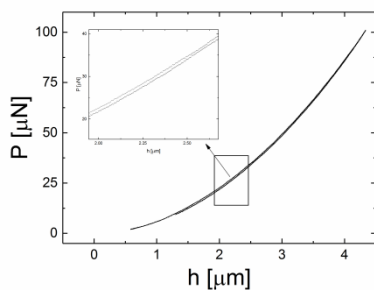


Fig. 2. Load-displacement curve of BEMA. Maximum applied load of 100 μN , reaching a maximum penetration depth of 4.34 μm . The sample reveals a purely elastic behavior as it recovers its initial position when the applied load (P) is removed.

B. Acoustic response

The acoustic response of the 3D-printed devices was tested by playing a frequency sweep from 300 Hz to 17 kHz, at amplitude of 3 V_{pp} using the set up shown in Fig. 3.

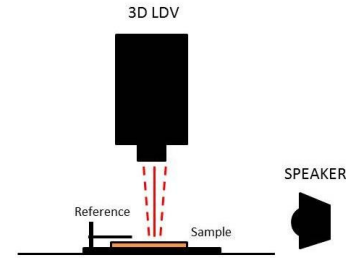


Fig. 3. Schematic set up to test the acoustic response of the 3D-printed samples. The loudspeaker sits behind the sample at a distance of 25 cm (far field), and the 3D-LDV head stays on top of the sample. The sample was fixed on the table, and a Bruel&Kjaer (B&K) 4138 microphone is used as a reference.

All the samples responded to higher frequencies in the thin part, and to lower frequencies in the thick part of the membrane. Afterwards, the response of the sample to single-frequency inputs was studied, revealing larger amplitude of motion in the thin part at higher frequencies, and larger amplitude of motion in the thick part at lower frequencies (Table I). Finite element analysis (FEA) suggested that the first and second modes correspond to 1.98 kHz, and 2.4 kHz respectively, which are in good accordance with the experimental results.

TABLE I. AVERAGE DISPLACEMENT VALUES (Z AXIS)

Sample	f [kHz]	Thick [nm]	Thin [nm]
1	1.4	0.84	0.78
	2.6	1.85	1.41
	8.5	0.09	0.30
	12	0.01	0.04
2	1.7	1.61	1.26
	2.69	1.12	1.05
	9	0.14	0.21
	12	0.019	0.021

C. Piezoelectric characterization

The output voltage was measured when the samples were excited at single frequencies within the range of 1 kHz to 17 kHz. Responses like the one shown in Fig. 4b were obtained for all the samples at all frequencies. Bursts consisting of 2 cycles and 100 ms, at amplitude of 20 V_{pp} were played, varying the distance between the loudspeaker and the sample from 35 cm to 10 cm in order to properly discern between the electromagnetic and acoustic response. Fig 4a shows the input signal at 15 kHz.

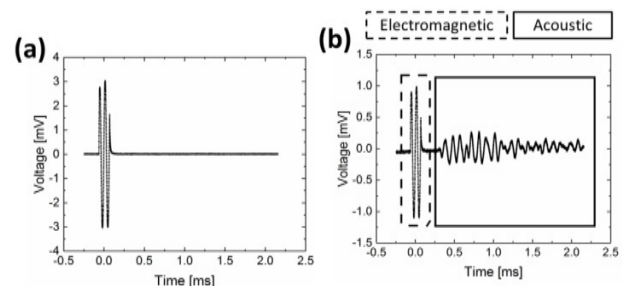


Fig. 4. (a) Shows the acoustic input signal at 15 kHz consisting of a burst of 2 cycles and 100 ms of duration, and (b) shows the response of the device, which is divided into the electromagnetic and the acoustic response. The same experiment was repeated for all the samples in the range of frequencies from 1 kHz up to 17 kHz.

After all the data was recorded, the ΔV of the acoustic signal was measured and normalized against the B&K microphone output. Measurements of sample 1 required a high pass filter to remove noise at 50 Hz, which was overlapping with the acoustic signal. Due to the nature of the filtering process, an amplifier was also needed, giving an amplification factor of 255, and 350 at 1 kHz, and 2 kHz respectively, and a factor of 475 from 3 kHz to 17 kHz. The normalized values obtained are shown in Fig. 5.

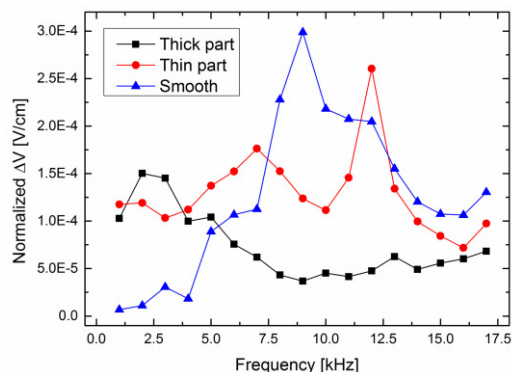


Fig. 5. Normalized values of the output voltage of the different measured devices when playing sound at different frequencies.

IV. CONCLUSIONS

The mechanical properties of the synthesized polymer have been studied by means of nanoindentation, and are in accordance with previous studies. Load-displacement curves showed that BEMA presents a purely elastic behaviour.

3D LDV experiments showed that the thick part of all the samples moves at a higher amplitude at low frequencies (from 1 kHz to 3 kHz) and the thin part moves at higher amplitudes when higher frequencies are played. The difference in amplitude was more noticeable in sample 1 than in sample 2 due to its geometry. As sample 1 has different regions of uniform thickness, the coupling between the thick and the thin region is lower, leading to higher amplitudes of motion at specific frequencies. This behaviour is similar to the locust's TM, where thinner regions of the membrane move at higher amplitudes at high frequencies and vice versa, leading to frequency selection.

Finally, the output voltage was measured at single frequency inputs and normalised using a B&K microphone as a reference. Sample 2 showed a better response at high frequencies (9 kHz), even though a small peak is observed at 3 kHz. Sample 1 showed two different tendencies according to the thick and thin regions. In the thick region, a better signal was obtained at low frequencies, revealing a peak between 2 kHz and 3 kHz, whereas the thin part of the device presented higher voltage amplitude at higher frequencies (7 kHz, and 12 kHz), leading to frequency selectivity of the devices.

It was also noted that the measured output voltage values are not linear with the mechanical displacement of the samples. This is because the PVDF films behave like capacitors, presenting high impedance values below 3 kHz, making it easier to obtain an electric signal at higher frequencies. This device is expected to work from room temperature up to 75-

80° C, which is the maximum usable temperature of the PVDF films, where losses in the d_{33} coefficients will take place due to the randomization of the dipoles. Furthermore, this is a first prototype and further investigation needs to be done to study its reproducibility.

This work revealed that simple bio-inspired devices can lead to systems able to discern between high and low acoustic frequencies. Further, the devices provided a good response at a broader range of frequencies. This work also gives an insight into the creation of functional 3D-printed sensors through a cheaper and more time-efficient process.

ACKNOWLEDGMENTS

The authors would like to thank Dr. Milovan Cardona for his guidance and help using the mechanical testing techniques at the University of Strathclyde Biomedical Engineering group.

REFERENCES

- [1] K. Haupt, and K. Mosbach, "Molecularly Imprinted Polymers and Their Use in Biomimetic Sensors", *Chem. Rev.*, vol. 100 (7), pp. 2495-2504, 2000
- [2] M. Shahinpoor, Y. Bar-Cohen, J. O. Simpson, and J. Smith, "Ionic polymer-metal composites (IPMCs) as biomimetic sensors, actuators and artificial muscles – a review", *Smart Mater. Struct.*, vol. 7 (6), pp. R15-R30, 1998
- [3] R. L. Ripley, and B. Bhushan, "Bioarchitecture: bioinspired art and architecture – a perspective", *Phil. Trans. R. Soc. A*, vol. 374, pp. 1-36, 2016
- [4] C. Sanchez, H. Arribart, and M. M. G. Guille, "Biomimeticism and bioinspiration as tools for the design of innovative materials and systems", *Nat. Mater.*, vol. 4, pp. 277-288, 2005
- [5] T. Nakata, H. Liu, Y. Tanaka, N. Nishihashi, X. Wang, and A. Sato, "Aerodynamics of a bio-inspired flexible flapping-wing micro air vehicle", *Bioinspir. Biomim.*, vol. 6 (4), pp. 045002, 2011
- [6] J. H. Long, N. M. Krenitsky, S. F. Roberts, J. Hirokawa, J. de Leeuw, and M. E. Porter, "Testing Biomimetic Structures in Bioinspired Robots: How Vertebrate Control the Stiffness of the Body and the Behavior of Fish-like Swimmers", *Integr. Comp. Biol.*, vol. 51 (1), pp. 158-175, 2011
- [7] M. Dijkstra, J. J. van Baar, R. J. Wiegernik, T. S. J. Lammerink, J. H. de Boer, and G. J. M. Krijnen, "Artificial sensory hairs based on the flow sensitive receptor hairs of crickets", *J. Micromech. Microeng.*, vol. 15 (7), pp. S132-S138, 2005
- [8] T. York, S. B. Powell, S. Gao, L. Kahan, T. Charanya, D. Saha, N. W. Roberts, T. W. Cronin, J. Marshall, S. Achilefu, S. P. Lake, B. Raman, and V. Gruev, "Bioinspired Polarization Imaging Sensors: From Circuits and Optics to Signal Processing Algorithms and Biomedical Applications", *Proc. IEEE*, vol. 102, pp. 1450-1469, 2014
- [9] Y.-L. Park, B.-R. Chen, D. Young, L. Stirling, R. J. Wood, E. Goldfield, and R. Nagpal, "Bio-inspired active soft ortotic device for ankle foot pathologies", *IEEE/RSJ International Conference on Intelligent Robots and Systems (IROS)*, pp. 4488-4495, 2011
- [10] J. F. C. Windmill, S. Bockenbauer, and D. Roberts, "Time-resolved tympanal mechanics of the locust", *J. R. Soc. Interface*, vol. 5 (29), pp. 1435-1443, 2008
- [11] J. F. C. Windmill, M. C. Göpfert, and D. Roberts, "Tympanal travelling waves in migratory locusts", *J. Exp. Biol.*, vol. 208 (1), pp. 157-168, 2005
- [12] W. C. Oliver, and G. M. Pharr, "An improved technique for determining hardness and elastic modulus using load and displacement sensing indentation experiments", *J. Mater. Res.*, vol. 7, pp. 1564-1583, 1992
- [13] I. Roppolo, A. Chiappone, A. Angelini, S. Stassi, F. Frascella, C. F. Pirri, C. Ricciardi, and E. Descrovi, "3D printable light-responsive polymers", *Mater. Horiz.*, 2017